



ELSEVIER

Available online at www.sciencedirect.com

SCIENCE @ DIRECT®

Nuclear Instruments and Methods in Physics Research A 518 (2004) 443–447

**NUCLEAR
INSTRUMENTS
& METHODS
IN PHYSICS
RESEARCH**
Section A

www.elsevier.com/locate/nima

MicroPattern gas detectors with pixel read-out

L. Latronico

INFN-sez. Pisa, V. Buonarroti 2, Pisa 56100, Italy

Abstract

MicroPattern Gas Detectors with pixel read-out are position-sensitive proportional counters obtained by coupling a gas amplifying stage to a pixel charge collection plane. Advanced PCB techniques, offering typical feature size of the order of a few microns, are used to construct the detectors, which show excellent spatial resolution and fast charge collection. In this paper it is shown how the design of the read-out system can maximize the intrinsic performance of these devices for two practical implementations, in the field of X-ray Astronomy and Plasma Imaging.

© 2003 Elsevier B.V. All rights reserved.

Keywords: MicroPattern; Position-sensitive detector; Pixel read-out

1. Introduction

A new era in gas detector development began when application of new construction technologies allowed definition of collecting electrodes with μm accuracy. Photolithography from microelectronics was applied to MSGC development, and advanced PCB techniques were used for MicroPattern Gas Detectors (MPGD) like GEM [1], Micro-Groove [2], CAT [3], WELL [4] and many others.

Gas detectors performances evolved towards solid state device standards (spatial resolution $\sim 30\ \mu\text{m}$, rate capability of a few MHz/mm^2), still keeping the distinctive properties of gaseous detectors like a light sensitive medium, sensitivity to X-rays and reasonably low production cost.

A very attractive class of MPGD is the one where a GEM detector is used as a charge-amplifying stage, completely decoupled from the readout electrodes, allowing use of a pixel read-out

pattern which can be optimized for the desired application.

Two examples of this approach are described in this paper, where we demonstrate how a careful design of the pixel geometry provides excellent resolving power and high rate capability that would be unavoidably lost by using a conventional projective read-out approach.

2. Applications

The basic detector for both applications is shown in Fig. 1. Primary charge from X-ray conversion in the first gap is drifted to the GEM plane, a $50\ \mu\text{m}$ Kapton foil, metal-clad on both sides and chemically pierced by a regular matrix of holes, typically $60\ \mu\text{m}$ in diameter and $90\ \mu\text{m}$ pitch. The high dipole field inside the holes created by application of a voltage gradient across the GEM starts an avalanche multiplication with proportional gains above 10^3 and generates a signal that can trigger the read-out electronics.

E-mail address: luca.latronico@pi.infn.it (L. Latronico).

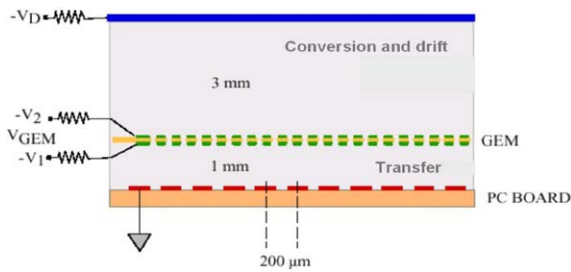


Fig. 1. View of a MicroPattern detector with pixel read-out.

Secondary electrons are then drifted to the read-out electrodes on the collection plane, that can be freely structured in pixels or pads to get full bi-dimensional reconstruction capability. The output signal is proportional to the charge collected by the read-out electrodes and is quite fast, being induced by the electrons drift in the transfer gap (~ 20 ns FWHM in a 1 mm gap).

2.1. X-ray astrophysical polarimetry

The aim of this application is to reconstruct photoelectron tracks produced in the gas by incoming X-rays.

The photoelectric effect is in fact very sensitive to photon polarization: the differential cross-section for a linearly polarized photon has a maximum in the plane orthogonal to the direction of the incoming photon and varies with θ (the polar angle) and ϕ (the azimuthal angle) as follows:

$$\frac{d\sigma}{d\Omega} = r_0^2 Z^5 \alpha^4 \left(\frac{m_e c^2}{h\nu} \right)^{7/2} \frac{4\sqrt{2} \sin^2 \theta \cos^2 \phi}{(1 - \beta \cos \theta)^4}. \quad (1)$$

Photoelectrons from polarized incoming X-rays are therefore preferentially ejected in the plane orthogonal to the photon, with $\cos^2 \phi$ modulation, so that polarization of the incoming radiation can be measured by the angular distribution of the emitted photoelectrons.

The charge collection plane of our detector is structured in a finely segmented, hexagonal pixel array with $200 \mu\text{m}$ pitch. The photoelectron track, of the order of 0.5 mm for the chosen Ne(80%)-DME(20%) gas mixture, can then be efficiently

sampled and reconstructed in two dimensions with a very good resolution. Moreover, the charge collected by each pixel is proportional to the primary clusters of charge released in the ionizing collisions occurred along the track, so that full reconstruction of the photoelectron energy loss dynamics is possible.

A typical event is shown in Fig. 2, where full development of the track can be followed. At the beginning of the track an Auger electron is emitted in a random direction, then the photoelectron travel in the direction of the electric field orientation until all the energy is released. In the last part of the track, the residual energy is deposited in few collisions (Bragg peak), and large Coulomb scattering with nuclei can occur, which randomize the track.

A specific reconstruction algorithm that relies on the central part of the track was developed. The absorption point is evaluated along the major principal axis of the charge distribution at a given distance from the barycentre. A new cluster of pixels is defined within a given distance from the impact point, and the principal axis of this distribution is the reconstructed photoemission [9].

The MPGD has been tested with unpolarized and polarized radiation; the angular distribution of the photoelectrons emitted in the two cases is shown in Fig. 3.

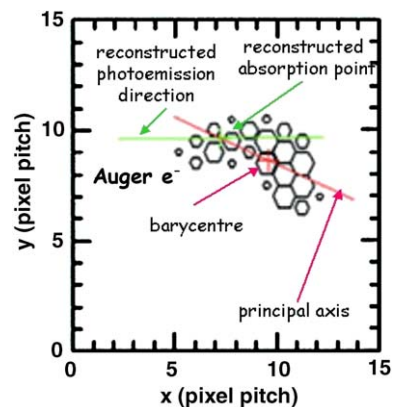


Fig. 2. Real photoelectron track. Reconstruction of the photoemission direction is done with the identification of the absorption point and the removal of the final part of the track, where directional information is lost due to track randomization Coulomb scattering.

As expected, the electric field for unpolarized radiation is randomly oriented, while the distribution for polarized radiation is peaked around the polarization angle and modulated with the characteristic \cos^2 term from the photoelectric effect cross-section, plus a constant term due to the randomization induced by Coulomb scattering.

A fundamental parameter in polarimetry is the so-called *modulation factor*, given by

$$\mu = \frac{C_{\max} - C_{\min}}{C_{\max} + C_{\min}} \quad (2)$$

The distribution of Fig. 3b has a modulation factor of $\sim 50\%$. Such a good performance was considered as a breakthrough for astrophysical polarimetry measurements, where a high degree of polarization is expected in the X-ray emission of most sources, but technological limitations never allowed conclusive measurements [5–8].

The modulation factor, together with detector efficiency, is used to define the Minimum Detectable Polarization (MDP), which is the minimum modulated flux needed to exceed the background and the signal from the unpolarized fraction of the source, at a given confidence level.

The tested prototype at the focus of the XEUS-1 space mission could perform polarimetry at 1% level, in the energy range 2–10 keV, on many bright AGN with about 1 day observation, corresponding to an improvement in sensitivity between one and two orders of magnitude with

respect to conventional Thomson or Bragg polarimeters.

2.2. Time-resolved plasma diagnostic

In this second application we have exploited the possibility of reading many individual pixels in parallel, each one operating as a free-running counter, to obtain very high global rate. We have developed a fast system for plasma imaging based on a pinhole camera coupled to a MPGD with a GEM as amplifying stage [10].

A sketch of the set-up with the detector positioned to get a tangential view of the hottest region of the plasma (1–10 keV) is shown in Fig. 4.

The read-out plane (2.5 cm^2) is equipped with a 2-D read-out PCB with 144 pixels of 2 mm^2 , as to contain the photoelectron range into a single pixel and avoid double-counting. The active area

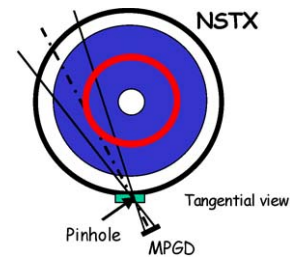


Fig. 4. Sketched view of the National Spherical Tokamak EXperiment set-up.

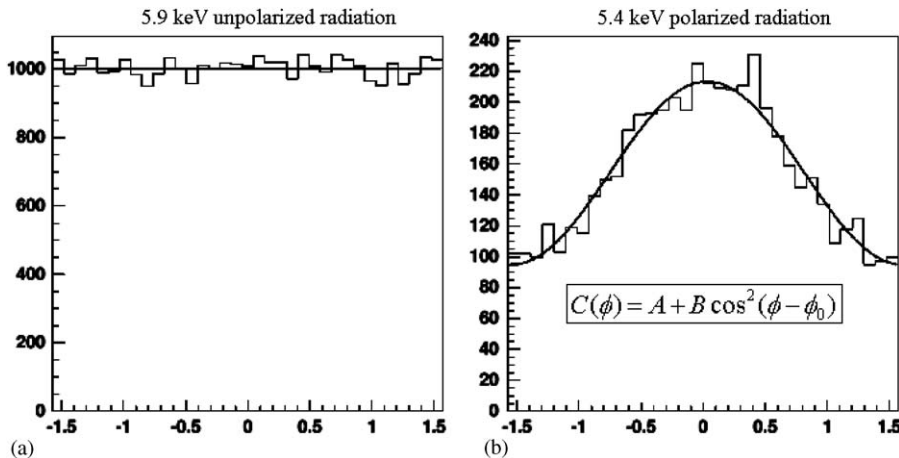


Fig. 3. Cluster angular distribution for unpolarized (a) and polarized radiation (b).

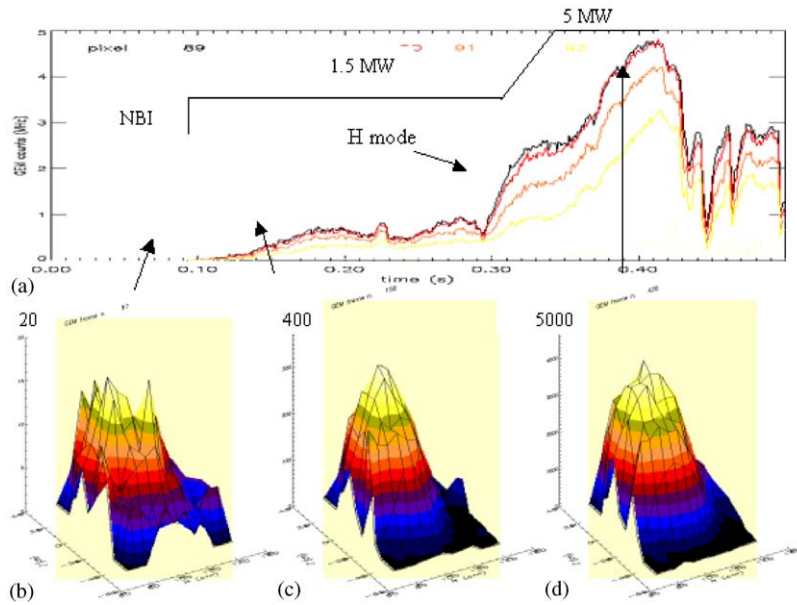


Fig. 5. Time history of some central pixels (framing rate 1 kHz).

roughly images 80 cm^2 of the plasma through the pinhole camera.

Each pixel has been individually energy calibrated to within 2% accuracy, so that energy discrimination is done by changing either the GEM voltage or the discriminator threshold. With a tangential view of the plasma, efficient energy discrimination is essential to isolate the contribution of the plasma core, extremely hotter than the surrounding area.

The pixel noise is about $2000e^-$, giving a S/N ratio of about 1000 at the highest emissivity.

The system can take images of the plasma at very high frame rate (up to 100 KHz), with a maximum counting rate before saturation of $10^7 \gamma/s \cdot \text{pixel}$, for a global rate of more than 10^9 Hz (dead time $\sim 170 \text{ ns}$). The dynamic range of the system is ~ 300 .

The time history of a few central pixels as power is injected into the system, is shown in Fig. 5, showing high oscillations in the last part of the injection. Images from the time development of the plasma core in critical conditions indicated deviations from the expected behavior, suggesting review of current models (see Fig. 6).

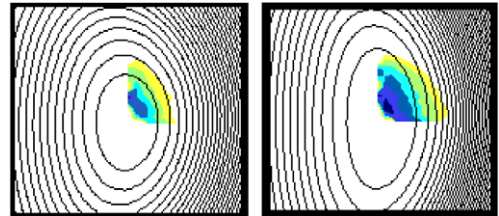


Fig. 6. Time development (0.5s) of the plasma core for a 5 MW, $\beta_p = 1.2$ injection; measurement and current models (isolines) do not match.

3. Conclusions

Two novel systems for X-ray polarimetry and plasma diagnostic have been developed by coupling a Micro Pattern Gas Detector with pixel read-out to a GEM used as amplifying stage. For both applications tailoring of the read-out pattern was crucial to exploit the high resolution offered by these devices in view of the specific application.

In the former case the high granularity of a low-pitch ($\sim 100 \mu\text{m}$) full-coverage hexagonal pixel array allowed one to efficiently reconstruct photoelectron tracks as short as $\sim 400\text{--}800 \mu\text{m}$. In the latter application, the extremely fast acquisition

(up to 100 kHz) obtained with a matrix of independent macropixels (2 mm^2) allowed following the time evolution of hot fusion plasmas.

References

- [1] F. Sauli, Nucl. Instr. and Meth. A 386 (1997) 531.
- [2] R. Bellazzini, et al., Nucl. Instr. and Meth. A 424 (1999) 444.
- [3] G. Chaplier, et al., Nucl. Instr. and Meth. A 426 (1999).
- [4] R. Bellazzini, et al., Nucl. Instr. and Meth. A 423 (1999) 125.
- [5] M.J. Rees, Mon. Not. Roy. Astron. Soc. 171 (1975) 457.
- [6] R.A. Sunyaev, L.G. Titarchuck, Astron. Astrophys. 143 (1985) 374.
- [7] Yu.N. Gnedin, G.G. Pavlov, Yu.A. Shibano, Sov. Astron. Lett. 4 (1978) 117.
- [8] E. Costa, P. Soffitta, R. Bellazzini, A. Brez, N. Lumb, G. Spandre, et al., Nature 411 (2001) 662.
- [9] R. Bellazzini, et al., A novel gaseous X-ray polarimeter: data analysis and simulation, Proceedings of SPIE 4843 (2003) 394.
- [10] D. Pacella, et al., X-VUV spectroscopic imaging with a micropattern gas detector, Nucl. Instr. and Meth. A 508 (2003) 414.